

# Fan-Beam Computerized Tomography Simulation

Kutay Ugurlu

**Abstract**—This project report demonstrates the implementation of Fan Beam Computerized Tomography simulation. The effect of different design parameters including the length of the detector, the number of beams and the angle between consecutive projections is inspected and discussed comparatively in both quantitative and qualitative manner. An improvement of 105% in structural similarity index is observed by utilizing the idea of convolution back projection. The work is derived from the previously developed code in Parallel Beam X-Ray Computerized Tomography [6]. The developed software and GUI to run it can be found in [github.com/kutay-ugurlu/Fan-Beam-Computerized-Tomography-Simulation](https://github.com/kutay-ugurlu/Fan-Beam-Computerized-Tomography-Simulation)

**Index Terms**—imaging, medical imaging, X-Ray computerized tomography, image reconstruction

## I. Introduction

The purpose of this project report is to demonstrate the procedure followed to simulate Fan-Beam Projected X-Ray Computerized Tomography. This project report consists of Theory, Implementation, Results and Discussion sections. The second section introduces the technical background for the CT simulation and the following section illustrates the algorithm using pseudocode snippets. Results and Discussion section presents the comparative results regarding different user-specified parameters with the conclusion and reasons behind them.

### A. History

The history of X-Ray Computerized Tomography can be dated back to 1917, when an Austrian mathematician called Johann Radon invented an algorithm, referred to as Radon transform today, on how to calculate line integrals in a two-dimensional section. The idea of computed tomography was developed in 1967 and was first used in a medical setting was in 1971 [2], by Godfrey Hounsfield. The device was tested at James Ambrose's department at Atkinson Morley Hospital in Wimbledon. This first model did not include a computer, instead the waves was written on a magnetic tape of the device EMI Scanner CT1010 in Figure 1. It was in 1973 that commercial CT scanners were available to the public. [5]

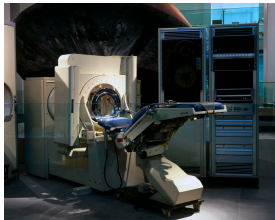


Fig. 1: First EMI Scanner [7]

## II. Theory

### A. X-Ray Attenuation

In X-ray tomography, images are modelled as attenuation coefficient distributions which is a measure of how much X-ray beams are attenuated when they propagate through an object. This problem can be modeled as in Eqn. 1 for an arbitrary object.

$$I_{measured} = I_0 e^{-\iiint_{object} \mu(x,y,z) dx dy dz} \quad (1)$$

When the object to be imaged is two-dimensional or can be reduced to a two-dimensional slice, Eqn 1 reduces to Eqn 2:

$$I_{measured} = I_0 e^{-\iint_{slice} \mu(x,y) dx dy} \quad (2)$$

### B. Radon Transform

Radon Transform computes the line integrals along the objects to obtain projections along an arbitrary angle  $\theta$  for an arbitrary beam  $t$ , using the formula given in Eqn. 3.

$$p_\theta(t) = \iint_{-\infty}^{\infty} \mu(x,y) \delta(x \cos(\theta) + y \sin(\theta) - t) dx dy \quad (3)$$

This equation models the X-ray beams as parallel lines through the object. In a more practical scenario, the X-ray source is modelled as a point source and beams are projected from source to the object in fan beam shape, due to the equiangular spaced discrete detector locations. This modelling can be achieved by introducing geometric transformation between projection variables.

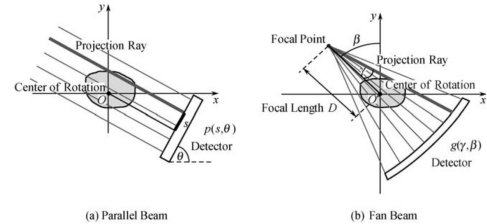


Fig. 2: Parallel Beams and Fan Beams [4]

In Figure 2b, the projection angle with respect to center of rotation is defined as  $\beta$  and the deviation from the center beam that is parallel to the  $\beta$  beam is defined as  $\gamma$  angles. In addition, the source to origin distance is labelled as  $D$ , resulting in source to detector distance of  $2D$ .

With source to detector distance redefined as  $D$  and the remaining quantities defined as above, one could transform the equation in 3 to 6 using Eqn. 4 and 5.

$$t = D \cdot \sin(\gamma) \quad (4)$$

$$\theta = \beta + \gamma \quad (5)$$

$$p_\beta(\gamma) = \iint_{-\infty}^{\infty} \mu(x, y) \delta(x \cos(\theta) + y \sin(\theta) - D \sin(\gamma)) d\gamma d\beta \quad (6)$$

### C. Fourier Slice Theorem

The Fourier slice theorem states that Fourier transform of a projection vector  $S_\theta(\omega) = \mathcal{F}(p_\theta(t))$  is the section of the original image distribution's Fourier transform  $\mathcal{F}(\omega, \theta)$  along the slice of angle  $\theta$ , which is formally described by Eqn. 7 [1].

$$S_\theta(\omega) = \mathcal{F}(\omega \cos \theta, \omega \sin \theta) \quad (7)$$

### D. Back Projection

According to Fourier Slice theorem, as it is formulated in [1], the original image distribution from projections can be obtained as follows:

$$f(x, y) = \int_0^\pi \left[ \int_{-\infty}^{+\infty} S_\theta(\omega) |w| e^{-j2\pi\omega t} d\omega \right] d\theta \quad (8)$$

The term  $|w|$  originates from the Jacobian of the coordinate transformation between Cartesian Space and Polar frequency variables.

$$f(x, y) = \int_{-\infty}^{+\infty} \int_{-\infty}^{+\infty} \mathcal{F}(u, v) e^{-j2\pi(u x + v y)} du dv \quad (9)$$

$$u = \omega \cos \theta \quad (10)$$

$$v = \omega \sin \theta \quad (11)$$

$$du dv = \omega d\omega d\theta \quad (12)$$

The factor  $\omega$  in Eqn. 12 derives from the Jacobian as follows:

$$J = \begin{vmatrix} \frac{\partial u}{\partial \omega} & \frac{\partial v}{\partial \omega} \\ \frac{\partial u}{\partial \theta} & \frac{\partial v}{\partial \theta} \end{vmatrix} = \begin{vmatrix} \cos \theta & \sin \theta \\ -\omega \sin \theta & \omega \cos \theta \end{vmatrix} \quad (13)$$

$$= \omega(\sin^2 \theta + \cos^2 \theta) = \omega \quad (14)$$

### E. Convolution Back Projection

Eqn. 8 tells us that the 1D Fourier transforms of the projection vectors should be weighted, i.e. filtered, with  $|w|$  to obtain the perfect reconstruction of the original unknown distribution. From Eqn. 8, one can deduce that the impulse response of the projection system is  $\frac{1}{|\omega|}$ , i.e., the components representing the high frequencies in the image distribution is attenuated when they are projected and represented in the Fourier space.

To overcome this low-pass effect, the projections should be filtered with the sequence having the frequency distribution  $|w|$ . The filter having the band-limited characteristics of above-mentioned frequency response is called Ram-Lak filter.

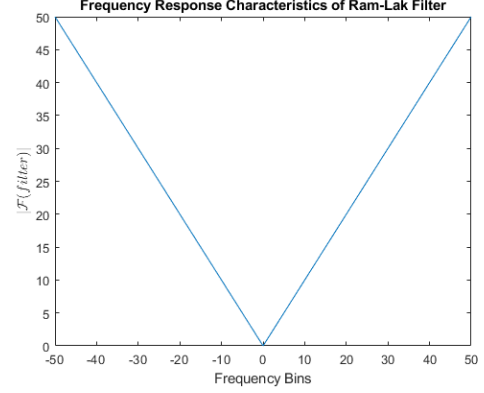


Fig. 3: Ram-Lak filter response

The sharp decrease in the Ram-Lak filter response causes ringing effect in the reconstructed images. To overcome this, the filter can be smoothed out in the higher frequency region with low-pass windows given in Figure 4

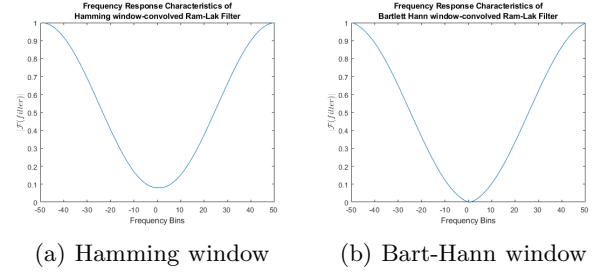


Fig. 4: Smoothing window functions

Then, the resultant filter responses are as follows:

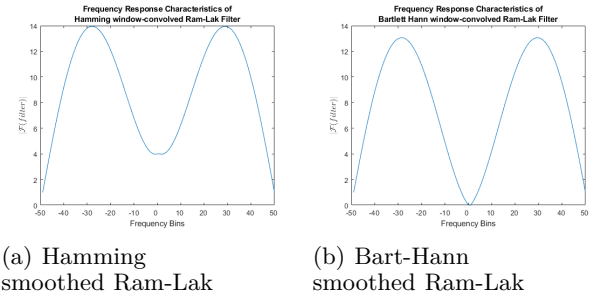


Fig. 5: Ram-Lak filter response smoothed out with window functions

The columns of the projection matrix of size  $[\#Rays \times \#ProjectionAngles]$  is convolved with the filters having the responses shown in Figure 5. This operation is called Convolution Back Projection.

### III. Implementation

In this section, the computer implementation of the scientific background explained in Section Theory is going to be described.

---

#### Algorithm 1 Projection algorithm

---

```

procedure Projection( $I, N_D, L_D, L_{SD}$ )
  Projections = ZEROS
  Form the image Grid  $[X(:), Y(:)]$ 
  for Projection angle  $\beta$  do
    for Fan beam angle  $\gamma$  do
       $\triangleright Line = F(x, y, \beta, \gamma)$ 
      Calculate x intersection
      Calculate y intersection
      Sort  $\triangleright$  Regular grid
      Find distance between intersections  $\triangleright$  weights
      Find the corresponding pixels
      Calculate projection  $\triangleright weights \cdot I(pixels)$ 
      Store in projection matrix
    end for
  end for
  return Projection matrix

```

---

The matrix returned by the procedure defined in Algorithm 1 is used in Algorithm 2 to reconstruct the image.

---

#### Algorithm 2 Back projection algorithm

---

```

procedure Projection( $I, N_D, L_D, L_{SD}$ )
  Projections = ZEROS
  Form the image Grid  $[X(:), Y(:)]$ 
  for Projection angle  $\beta$  do
    for Fan beam angle  $\gamma$  do
       $\triangleright Line = F(x, y, \beta, \gamma)$ 
      Calculate x intersection
      Calculate y intersection
      Sort  $\triangleright$  Regular grid
      Find distance between intersections  $\triangleright$  weights
      Find the corresponding pixels  $\triangleright$  Mid-points
      Sum projections in the pixels  $\triangleright I(pixel) + =$ 
         $projection$ 
    end for
  end for
  return Reconstructed Image

```

---

The developed application implements the above algorithms in order to project and reconstruct the image. All components of the software and the Graphical User Interface is implemented in MATLAB(The MathWorks®, Inc., Natick, Massachusetts, United States.) The guide to how to use the graphical user interface can be achieved in the README section of the following repository: [github.com/kutay-ugurlu/Fan-Beam-Computerized-Tomography-Simulation](https://github.com/kutay-ugurlu/Fan-Beam-Computerized-Tomography-Simulation).

### IV. Results

Using the algorithm defined in the Implementation section, all the sample phantoms are reconstructed via Projection and Convolution Back projection algorithm. Figures 6 to 9 are reconstructed utilizing the following projection parameters for angles  $0^\circ, 45^\circ, 90^\circ$ :

- Number of detectors = 71
- Number of fans = 180
- Source to detector distance = Image size  $\times \sqrt{3}$
- Length of the detector = Source to detector distance
- Filter: Hamming

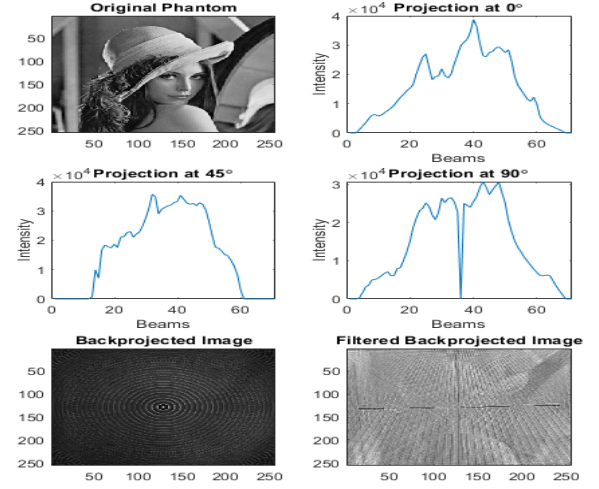


Fig. 6: Projections and reconstructions of Lena phantom

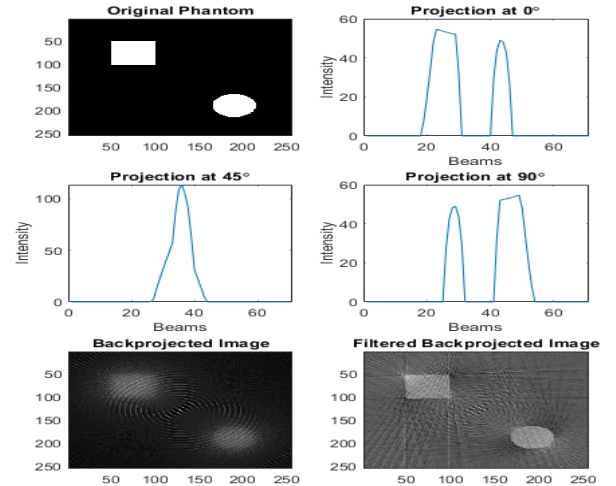


Fig. 7: Projections and reconstructions of Square-Circle phantom

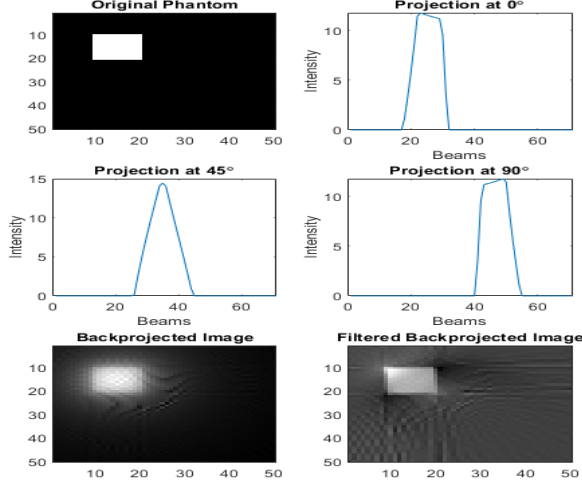


Fig. 8: Projections and reconstructions of Square phantom

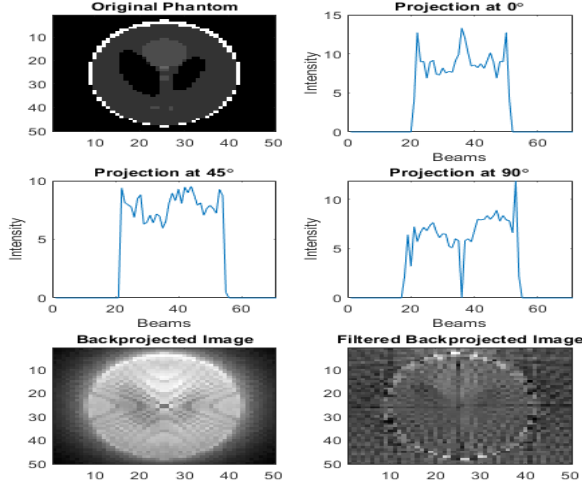


Fig. 9: Projections and reconstructions of Shepp Logan phantom

In addition, the effect of the parameters such as filter type, projection angle step size and number of detectors are examined using the structural similarity index [3] between the gray intensity pictures of ground truth phantoms and reconstructed images. The results of these experiments are presented in Tables I to III.

Phantoms		Shepp Logan	Square	Square Circle
Filters				
No-filter		0.153	0.100	0.029
Ram-Lak		0.231	0.057	0.032
BartHann		0.246	0.058	0.044
Hamming		0.244	0.058	0.043

TABLE I: SSIM Index for different filter reconstructions

Square circle phantom is utilized in the projection angle step size and number of detectors experiments due to the easiness of visual assessment and its having large number of pixels among the available samples.

Beams		50	75	150	300
Filters					
No-filter		0.015	0.018	0.017	0.035
Ram-Lak		0.019	0.019	0.024	0.039
BartHann		0.027	0.028	0.034	0.048
Hamming		0.026	0.028	0.033	0.048

TABLE II: SSIM Index for different number of beams

Angles		2	1	0.5	0.25
Filters					
No-filter		0.022	0.029	0.030	0.030
Ram-Lak		0.025	0.032	0.039	0.043
BartHann		0.028	0.044	0.049	0.048
Hamming		0.027	0.043	0.048	0.048

TABLE III: SSIM Index for different angles

The experiments show that the imaging parameters may affect the reconstructed imaging quality significantly with respect to the case where the parameters are not carefully selected. One example image reconstructed with  $0.5^\circ$  angle step size and 200 detectors can be seen in Figures 10 and 11.

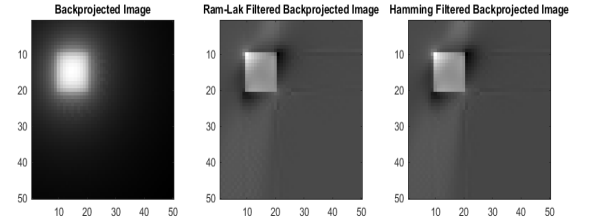


Fig. 10: Improved reconstruction of Square phantom

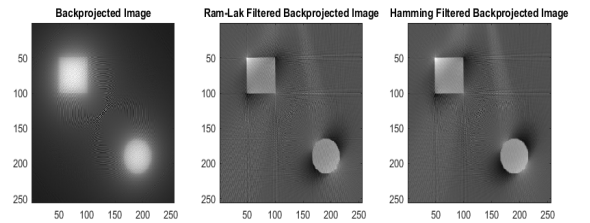


Fig. 11: Improved reconstruction of Square Circle phantom

## V. Discussion

A series of experiments are conducted to observe the effect of different imaging parameters in fan-beam X-ray computerized tomography setup. The results of the regarding experiments are shared in the Results Section. This section is devoted evaluate the results both quantitatively and qualitatively.

### A. Convolution Back Projection filter

A series of filters and windows are used in convolution back projection implementation to overcome the low-pass effect of the back projection algorithm described in Section II-E. The reconstruction similarity metrics in Table I show that the proposed filters can increase the similarity metric up to by 60% with respect to the metrics obtained by plain back projection algorithm for 3 of the 4 phantoms. This relation was not observed in the square phantom. The reason can be attributed to the fact that ringing effects (pixelation) caused by the filters decreases structural similarity in the regions further from the main object, although they increase the contrast by their high frequency characteristics.

### B. Number of Beams - Number of Detectors

X-Ray CT systems are considered to be overdetermined linear systems, due to high number of equations introduced by each X-ray beam compared to the number of pixels to be reconstructed. Table II shows that increasing the number of beams, hence increasing the number of measurements, may result in an increase of up to 105% in the similarity index. The theoretical explanation is that reconstructions with less error is possible in the higher dimension of measurements.

### C. Projection Angle Step Size - Number of Fans

The same relationship observed in the case of increasing number of beams is encountered in the case of increased number of fans. Table III shows that more number of fans may increase the similarity index by 78%. The reason behind this is that increasing the number of fans increases the number of measurement, as it is described Section V-B,

### D. Qualitative Assessment

In figures figs. 6 to 11, it is possible to observe an increasing contrast and quality of reconstructed images when convolution back projection algorithm is used. It is clear that introduction of these filters into the algorithm removes introduced by back projection.

## References

- [1] A. C. Kak and M. Slaney, "Principles of computerized tomographic imaging," in SIAM, 2001, pp. 56–65.
- [2] C. Richmond, Sir godfrey hounsfield, 2004.
- [3] Z. Wang, A. C. Bovik, H. R. Sheikh, and E. P. Simoncelli, "Image quality assessment: From error visibility to structural similarity," IEEE transactions on image processing, vol. 13, no. 4, pp. 600–612, 2004.
- [4] G. L. Zeng, "Image reconstruction: Applications in medical sciences," in Walter de Gruyter GmbH & Co KG, 2017, pp. 51–52.
- [5] ISCT, Half a century in ct: How computed tomography has evolved, Jul. 2018. [Online]. Available: <https://www.isct.org/computed-tomography-blog/2017/2/10/half-a-century-in-ct-how-computed-tomography-has-evolved#:~:text=Increased%20power%20and%20availability%20of,Laboratories%20using%20x%20ray%20technology..>
- [6] K. Ugurlu, "Parallel beam x-ray computerized tomography," 2020.
- [7] Emi ct brain scanner: Science museum group collection. [Online]. Available: <https://collection.science-museum-group.org.uk/objects/co134790/emi-ct-brain-scanner-ct-scanner>.